Progress In Electromagnetics Research M, Vol. 18, 143–157, 2011

A HYBRID HIGHER ORDER FDTD SCHEME FOR MODELING RADAR CROSS SECTION OF ELECTRICALLY LARGE TARGETS

X. Ai[1, *], Y.-P. Han[2], Z.-Y. Chen[2], and X.-W. Shi[1]

[1]Science and Technology on Antenna and Microwave Laboratory, Xidian University, Xi'an, Shaanxi 710071, China

[2]School of Science, Xidian University, Xi'an, Shaanxi 710071, China

Abstract—This paper proposes a hybrid higher order finite difference time domain (FDTD) scheme that combines the classical FDTD scheme and the higher order FDTD scheme with second order accuracy in time and fourth order accuracy in space for analyzing the three-dimensional electrically large scattering problems. The classical FDTD stencils were used as buffers in the scattered field region to make the higher order FDTD stencils not intrude inside the absorbing boundary condition's regions. The superior performance of the hybrid higher order FDTD scheme has been compared with the classical FDTD one. Numerical results demonstrate that the proposed scheme would improve the accuracy and save the computer resources significantly compared to the classical FDTD scheme involved in the radar cross section (RCS) calculation. The obtained computational efficiency allows this proposed scheme to model the RCS of electrically large targets using the number of higher order FDTD cells which are much less than that of the classical FDTD cells required by three-dimensional FDTD scheme.

1. INTRODUCTION

RCS is the measurement of a target's ability to reflect radar signals in the direction of a target's receiver. Generally, since the experimental measurement for a real-life experiment costs too much time and investment, and the application of Mie theory [1] was limited only to sphere and cylinder, the RCS are usually evaluated through numerical methods. The FDTD [2, 3] scheme has been widely used to solve

Received 29 April 2011, Accepted 19 May 2011, Scheduled 27 May 2011

* Corresponding author: Xia Ai (xai@mail.xidian.edu.cn).

Maxwell equations in several contemporary problem, such as scattering from electrically large or multiple targets, antenna array modeling, etc. Unfortunately, the performance of classical FDTD scheme, when calculating RCS, is not good enough, especially for electrically large target problems. In [4], the authors have validated classical FDTD scheme to model RCS of electrically large metallic targets. As mentioned in [5], errors in the RCS calculation can be mainly attributed to the source that the numerical error in calculating the near-field components used for near to far field transformation. In [5], Li et al. used a simple method to overcome the inaccuracy of the FDTD scheme calculating the backscattered RCS obtained with a monostatic radar. However, this method is not adaptable to the bistatic RCS when the target illuminated by a monochromatic electromagnetic wave, due to one of the virtual integration surface [6] has been removed. Therefore, an alternative way to improve the accuracy of the bistatic RCS is to reduce the numerical error in calculating the near-field components used for near to far field transformation.

The numerical dispersion is the dominant numerical error of classical FDTD scheme and poses a serious problem for the classical FDTD scheme when encountering electrically large targets. The spatial resolution for classical FDTD scheme has to be extremely fine to confine the total accumulated phase error within an acceptable level. However, the extremely fine spatial resolution should yield large computational domains and require significant computer resources, such as memory and execution time. Consequently, spatial resolution refinement is not an efficient solution and sometimes is not even possible for electrically large problems. Numerous methods have been developed to decrease the phase error, and the main developed methods of interest for this field were detailed analyzed by Shlager and Schneider in [7]. A correction for the phase error can be obtained by perturbing the space derivative by a factor which is different from unity in the classical second-order FDTD method so that the phase errors at some angles are reduced to zero at specific resolution and frequency [3]. Nehrbass et al. [8] optimize the phase error by modifying the phase velocity to decrease the error result from dispersion. Cole [9] improves the classical FDTD scheme using a nonstandard finite difference operator in which a correction function is used to minimize the errors between the analytic derivative and the new operator. Kim et al. [10] use a isotropic dispersion(ID) FDTD algorithm to improve the accuracy of classical FDTD scheme. Besides these methods which involved in second-order technology mentioned above, higher order FDTD schemes [5, 11–17] provide more appropriate choices. Although larger spatial stencils and more floating point

operations (FLOPS), such approaches overwhelm the second-order technique, because they require coarser meshes for a specific error level. Therefore, the higher order FDTD schemes could significantly decrease the computer resources, especial for electrically large problems.

Unfortunately, it is not convenient to implement the higher order FDTD schemes for the practical application which referring to the scattering problem because of the larger stencils compared to the classical FDTD schemes. These stencils could make the higher order FDTD schemes powerless due to the material discontinues caused by the absorbing boundary conditions, therefore, the stencils close to absorbing boundary regions should be carefully treated. Traditionally, this problem is dealt with by applying classical FDTD cells as special stencils [17, 18] between the higher order FDTD cells and the absorbing boundary regions, these special stencils could make the higher order FDTD cells do not intrude inside the absorbing boundary condition's regions, and can be only one layer classical FDTD cells. These hybrid scheme has been used to model electrically large waveguide problem [17] which referring to PEC boundaries in three-dimensional case. Unfortunate, the applications of this hybrid scheme have not been related to investigating the RCS of three-dimensional electrically large targets. In this paper, the Fang's [19] higher order FDTD scheme that is second order accuracy in time and fourth order accuracy in space scheme has been opted to calculate the RCS of electrically large targets, due to its simpler coefficient and less stencils compared to the several modified higher-order FDTD schemes [14, 16, 20]. The special stencils mentioned above have been introduced in the scattered field region to avoid that the higher order FDTD cells do not locate inside the second order perfect matched layers (PMLs) [21]. The RCS of electrically large sphere has been modeled, which has been compared with the Mie theory [1]. The numerical results demonstrate the proposed method should significantly improve the accuracy compared to the classical FDTD scheme using the same spatial resolution when involved in electrically large scattering problem. In addition, the proposed method could save a lot of computer resources compared to the classical FDTD scheme while keeping the same accurate level.

2. REVIEW OF THE HIGHER ORDER FDTD SCHEME

Although there are several higher order FDTD schemes, the Fang's [19] second order accuracy in time and fourth order accuracy in space which denoted as FDTD (2, 4) has been chosen as the basic scheme for the electrically large scattering problem in this paper. This due to the three factors: 1) the higher order scheme which is fourth order accuracy in

time and fourth order accuracy in space [22] demand extra variables to store the previous electric and magnetic fields in computational domain, and this would lead to more memory costs, 2) the higher order scheme which is second order accuracy in time and sixth or higher order in space would result in too large spatial stencils to dealt with in boundaries including absorbing boundaries and PEC boundaries, 3) the higher order schemes which are modified by introducing tuning factors to reduce the dispersion errors [17, 20, 23] would induce large spatial stencils which is similar to 2), however, the accurate level has not been improved significantly which would been shown in the two-dimensional experiment in Section 4.

For simplicity, we consider a source-free lossless homogeneous isotropic and three-dimensional medium. Maxwell's equations can be written as

$$\nabla \times \vec{H} = \varepsilon_0 \varepsilon_r \frac{\partial \vec{E}}{\partial t} \tag{1}$$

$$\nabla \times \vec{E} = -\mu_0 \mu_r \frac{\partial \vec{H}}{\partial t} \tag{2}$$

where ε_0 and μ_0 are the permittivity and permeability in free space, and the ε_r and μ_r are the relative permittivity and permeability of the medium.

The above equations will be discretized on a staggered grid as in the Yee's FDTD scheme [2]. The scheme should be correctly centered in both time and space, for deriving conservative difference formulas. Appling a Taylor series expansion, the following could be obtained

$$E_x \Big|_{i+0.5,i,k}^{n+1} = E_x \Big|_{i+0.5,i,k}^{n} + \Delta t \frac{\partial E}{\partial t} \Big|_{i+0.5,j,k}^{t=(n+0.5)\Delta t} \tag{3}$$

which is second order accuracy in time and time centered for the time derivative. Substituting (1) into (3), we obtain

$$E_x \Big|_{i+0.5,j,k}^{n+1} = E_x \Big|_{i+0.5,j,k}^{n} + \frac{\Delta t}{\varepsilon_0 \varepsilon_r} \left(\frac{\partial H_z}{\partial y} - \frac{\partial H_y}{\partial z} \right) \Big|_{i+0.5,j,k}^{t=(n+0.5)\Delta t} \tag{4}$$

Using a second order central difference approximation for both of the spatial derivatives, the classical Yee's FDTD scheme would be obtained. For simplicity, the second order spatial centered difference operators D_{2y} in y direction and D_{2z} in z direction has been defined as

$$D_{2y} F(i+0.5, j, k) = \frac{1}{\Delta y} \left[F \,|_{i+0.5,j+0.5,k} - F \,|_{i+0.5,j-0.5,k} \right] \tag{5}$$

$$D_{2z} F(i+0.5, j, k) = \frac{1}{\Delta z} \left[F \,|_{i+0.5,j,k+0.5} - F \,|_{i+0.5,j,k-0.5} \right] \tag{6}$$

then the classical Yee's formula for E_x can be written as

$$E_x\left|_{i+0.5,j,k}^{n+1}\right. = E_x\left|_{i+0.5,j,k}^{n}\right. + \frac{\Delta t}{\varepsilon_0\varepsilon_r} D_{2y} H_z^{n+0.5}(i+0.5,j,k) - \frac{\Delta t}{\varepsilon_0\varepsilon_r} D_{2z} H_y^{n+0.5}(i+0.5,j,k) \quad (7)$$

The fourth order central difference approximations for the spatial derivatives could be derived by using a Taylor's series approach. Let's consider the Taylor's series expansions

$$f\left(x \pm \frac{1}{2}\Delta\right) = f(x) + \left(\pm\frac{1}{2}\Delta\right)\frac{\partial}{\partial x}f(x) + \frac{1}{2!}\left(\pm\frac{1}{2}\Delta\right)^2\frac{\partial^2}{\partial x^2}f(x) + \frac{1}{3!}\left(\pm\frac{1}{2}\Delta\right)^3\frac{\partial^3}{\partial x^3}f(x) + O\left(\left(\pm\frac{1}{2}\Delta\right)^3\right) \quad (8)$$

$$f\left(x \pm \frac{3}{2}\Delta\right) = f(x) + \left(\pm\frac{3}{2}\Delta\right)\frac{\partial}{\partial x}f(x) + \frac{1}{2!}\left(\pm\frac{3}{2}\Delta\right)^2\frac{\partial^2}{\partial x^2}f(x) + \frac{1}{3!}\left(\pm\frac{3}{2}\Delta\right)^3\frac{\partial^3}{\partial x^3}f(x) + O\left(\left(\pm\frac{3}{2}\Delta\right)^3\right) \quad (9)$$

then, from (8) and (9), we can obtain

$$\frac{\partial}{\partial x}f(x) = \frac{9}{8}\left(\frac{f\left(x+\frac{1}{2}\Delta\right) - f\left(x-\frac{1}{2}\Delta\right)}{\Delta}\right) - \frac{1}{24}\left(\frac{f\left(x+\frac{3}{2}\Delta\right) + f\left(x-\frac{3}{2}\Delta\right)}{\Delta}\right) \quad (10)$$

Similar as (5) and (6), the fourth order spatial centered difference operators D_{4y} in y direction and D_{4z} in z direction has been defined as

$$D_{4y}F(i+0.5,j,k) = \frac{9}{8}D_{2y}F(i+0.5,j,k) - \frac{1}{24\Delta y}\left[F\left|_{i+0.5,j+1.5,k} - F\right|_{i+0.5,j-1.5,k}\right] \quad (11)$$

$$D_{4z}F(i+0.5,j,k) = \frac{9}{8}D_{2z}F(i+0.5,j,k) - \frac{1}{24\Delta z}\left[F\left|_{i+0.5,j,k+1.5} - F\right|_{i+0.5,j,k-1.5}\right] \quad (12)$$

Replacing the spatial derivatives in (4) with the fourth order difference approximations (11) and (12), we can derive the fourth order difference

formula based on the Yee space.

$$E_x\Big|_{i+0.5,j,k}^{n+1} = E_x\Big|_{i+0.5,j,k}^{n} + \frac{\Delta t}{\varepsilon_0\varepsilon_r} D_{4y} H_z^{n+0.5}(i+0.5,j,k) - \frac{\Delta t}{\varepsilon_0\varepsilon_r} D_{4z} H_y^{n+0.5}(i+0.5,j,k) \quad (13)$$

the other electric and magnetic field components can be derived using a similar manner.

Figure 1 shows the construction of the FDTD (2, 4) scheme that used for calculating E_x component based on Yee's lattice at the plane indexed $x + 0.5$. However, the FDTD (2, 4) scheme is still second order accuracy in time, but fourth order accuracy in space. Besides the four magnetic field components at the adjacent grids used in the Yee's scheme, there are extra four once-removed grids used in the FDTD (2, 4) scheme, as shown in Figure 1. The 'single arrow' denotes the grids used in the Yee's scheme, and the 'double arrow' denotes the extra four once-removed grids. It should be noted that, the spatial stencils of the FDTD (2, 4) become larger compared to the Yee's scheme, which would lead to be troublesome to deal with the PEC and absorbing boundary conditions. In addition, since the FDTD (2, 4) is based on Yee's lattice and the difference between the Yee's (referred to FDTD (2, 2)) and the FDTD (2, 4) scheme is just different spatial stencils, it is very easy to

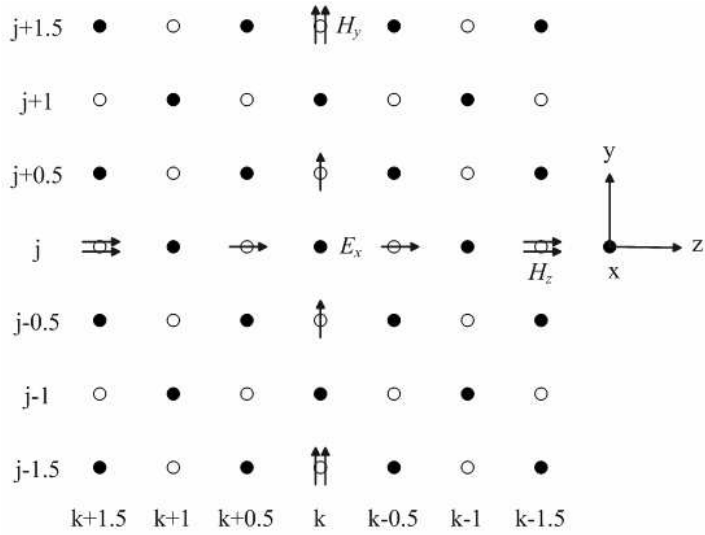

Figure 1. Construction of the FDTD (2, 4) scheme used for calculating E_x.

introduce the FDTD (2, 4) scheme into Yee's FDTD scheme computer code.

Following the example of Talflove and Hagness [3] the dispersion relation and stability criterion for the FDTD (2, 4) scheme are obtained

$$\left(\frac{1}{c\Delta t}\right)^2 \sin^2\left(\frac{\omega\Delta t}{2}\right) = \left(\frac{1}{\Delta x}\right)^2 \left[\frac{9}{8}\sin\left(\frac{k_x\Delta x}{2}\right) - \frac{1}{24}\sin\left(\frac{3k_x\Delta x}{2}\right)\right]^2 + \left(\frac{1}{\Delta y}\right)^2 \left[\frac{9}{8}\sin\left(\frac{k_x\Delta y}{2}\right) - \frac{1}{24}\sin\left(\frac{3k_x\Delta y}{2}\right)\right]^2 + \left(\frac{1}{\Delta z}\right)^2 \left[\frac{9}{8}\sin\left(\frac{k_z\Delta x}{2}\right) - \frac{1}{24}\sin\left(\frac{3k_z\Delta x}{2}\right)\right]^2 \quad (14)$$

where c is the velocity of the light in free space, ω is the wave angular frequency, $k_x = k\sin\theta\cos\varphi$, $k_y = k\sin\theta\sin\varphi$, $k_z = k\cos\theta$, k is the numerical wave number, θ and φ are the usual unit components in the spherical coordinate, which denote the wave propagation direction. To investigate the numerical dispersion characteristic of the FDTD (2, 2) scheme and the FDTD (2, 4) scheme, the parameters are choose as: $\omega = 2\pi \times 3 \times 10^8$ rad/s, $\Delta x = \Delta y = \Delta z = 0.05$ m, $\Delta t = 0.4949\Delta x/c$. Then, the numerical phase velocity v_p could be obtained by $v_p = \omega/k$.

Figure 2 compares the numerical phase velocity with overall propagation directions in both three-dimensional FDTD (2, 2) scheme and FDTD (2, 4) scheme. It is obvious that the phase velocity of the FDTD (2, 4) scheme is much closer to the velocity of the light in free

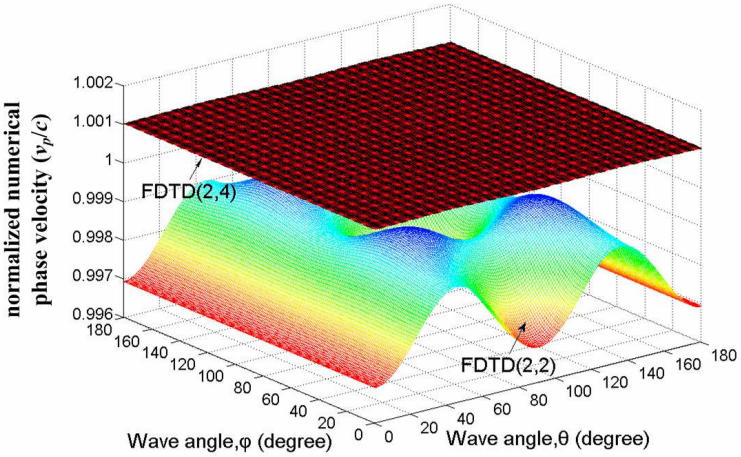

Figure 2. Numerical phase velocity with overall propagation directions.

space than the FDTD (2, 2) scheme in overall propagations, which means the physical phase-velocity error [3] of the FDTD (2, 4) scheme is much less than the FDTD (2, 2) scheme. In addition, the surface of the FDTD (2, 4) scheme in Figure 2 is much smoother than the FDTD (2, 2) scheme, which means the velocity-anisotropy error [3] of the FDTD (2, 4) scheme is more less than the FDTD (2, 2) scheme.

The stability bound for the three-dimensional versions of the scheme can be given [3]

$$\Delta t \leq \frac{(6/7)}{c\sqrt{\frac{1}{(\Delta x)^2}+\frac{1}{(\Delta y)^2}+\frac{1}{(\Delta z)^2}}} \tag{15}$$

Obviously, the maximum Δt permitted for the stability of the FDTD (2, 4) scheme is 6/7 of the corresponding limit for the Yee's scheme.

3. HYBRID FDTD (2, 4) SCHEME

However, as mentioned in previous section, there is a serious obstacle between the FDTD (2, 4) scheme and practical application referred to analyzing the scattering problems due to its larger spatial stencils compared to the FDTD (2, 2) scheme. These stencils would make the scheme inability to model material discontinues such as PEC boundary condition and absorbing boundary condition. The second order subgirdding technology has been used to successfully deal with the problem [18]. The second order subgirdding technology demand extra memories to store the electric and magnetic fields components obtained in the previous time steps, therefore, the technology is not a efficient way to solve the problem result from the larger stencils of the FDTD (2, 4) scheme. In [17, 24], an alternative but more efficient hybrid FDTD (2, 4) scheme which has been applied to handle the PEC boundary condition is to use a few FDTD (2, 2) scheme's stencils around the conducting objects and the FDTD (2, 4) scheme's stencils everywhere else in the modeled domain. More everthis method is simpler to implement than the subgirdding technology, and could reduce the memory and execution time cost.

In this paper, a similar method is used to handle the problem rooted in the larger stencils of the FDTD (2, 4) scheme encroach into the absorbing boundary condition's regions. The FDTD (2, 2) scheme's stencils as buffers are introduced into the outer boundary of scattered field regions. Figure 3 shows the construction of hybrid FDTD (2, 4) lattice based on the Yee's scheme. These buffers which made the FDTD (2, 4) scheme's stencils do not intrude inside the PML' regions can be only one FDTD (2, 2) scheme's cell thick. It should be pointed out that the negative influence of these buffers on the overall accuracy could be

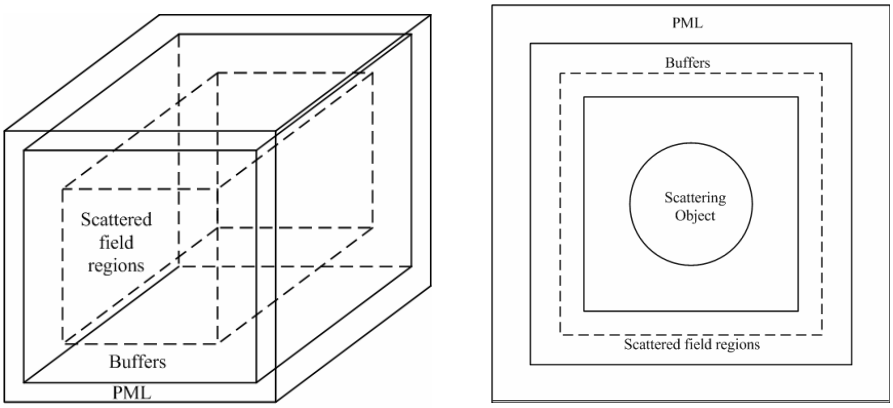

Figure 3. The construction of hybrid FDTD lattice. (a) 3-D view. (b) 2-D view at the top plane.

very little due to the numbers of these buffers are restricted to a few cells. Furthermore, this hybrid FDTD (2, 4) scheme guarantee the FDTD (2, 4) scheme more convenient to add in the existing computer code compared to the subgirdding technology. Usually, it only need to change a few codes to implement this scheme.

4. NUMERICAL RESULT

In this section, two experiments which refer to fundamental problems in RCS calculation are given to demonstrate validation of the proposed method in this work. The Mie series [1] are served as a benchmark date in both experiments. The monochromatic plane wave excitation has been used in both the example, which defined as follow

$$E_{inc} = \begin{cases} 0 & t < 0 \\ E_0 \sin(\omega t) & t \geq 0 \end{cases} \tag{16}$$

where, ω is the angular frequency of the incident wave.

Firstly, the performances of the modified FDTD (2, 4) [20, 23] scheme and the FDTD (2, 4) scheme used in this work for calculating the RCS in two-dimension case will be compared in order to illustrate the discussions in Section 2. The angular frequency of the incident wave is $\omega = 2\pi \times 3 \times 10^8$ rad/s, which corresponding to wavelength $\lambda_0 = 1$ m in free space. The direction of the incident plane wave is $\varphi = 0$, where φ is the angle between incident direction and the x-axis. The infinite cylinder with radius $a = 2\lambda_0$ located at the center of the

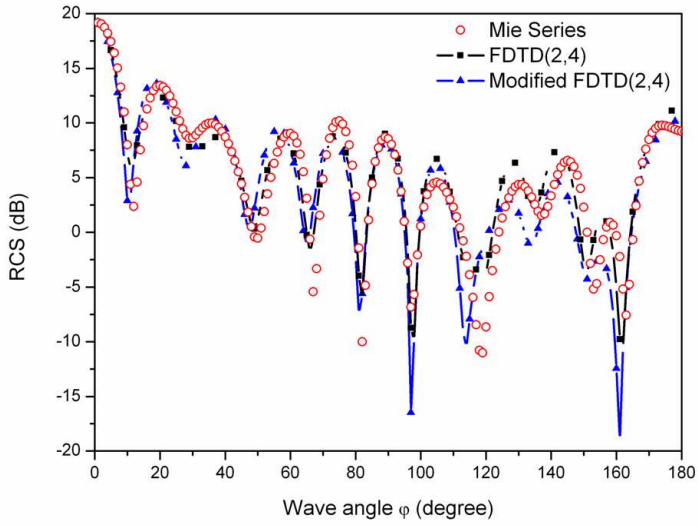

Figure 4. Comparison of the modified FDTD (2, 4) and FDTD (2, 4) scheme.

plane. The parameters for both of the schemes have been chosen as: CPW = 20, $\Delta x = \Delta y = \lambda_0/\text{CPW}$, $\Delta t = 0.5\Delta x/c$, where CPW is the number of cells per wavelength. The thickness of PML is 10 cells. The comparison of the two scheme has been shown in Figure 4. It can been see that the modified FDTD (2, 4) scheme do not improve the accuracy significantly referred to RCS calculation.

Then, we investigate the performance of the hybrid FDTD (2, 4) scheme for RCS calculation in three-dimensional case compared to the FDTD (2, 2) scheme. All the calculations are carried at a HP Workstation with 3.0 GHz CPU and 72 GB memory. The angular frequency of the incident wave is $\omega = 2\pi \times 3 \times 10^8$ rad/s, which is corresponding to wavelength $\lambda_0 = 1$ m in free space. The direction of incident plane wave is $\theta = 0$, $\varphi = 0$, where θ and φ are the usual unit components in the spherical coordinate, which means the direction is along z-axis in Cartesian coordinate. The radius of the dielectric sphere is $R = 10\lambda_0$, and the relative permittivity of the sphere is $\varepsilon_r = 4.0$. For this simulation, CPW = 20, $\Delta x = \Delta y = \lambda_0/\text{CPW}$ for both of the two schemes. $\Delta t = 0.5\Delta x/c$ and $\Delta t = 0.4949\Delta x/c$ for the FDTD (2, 2) scheme and the hybrid FDTD (2, 4) scheme respectively. The thickness of PML is 10 cells, which would minimize the errors caused by the reflection from the outer boundaries.

The results have been shown in Figure 5. It is clear that the hybrid

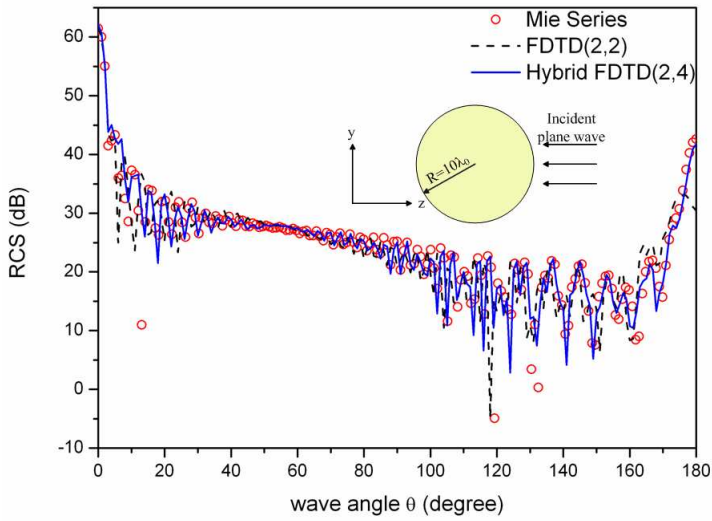

Figure 5. Copolarized RCS of dielectric sphere with radius $R = 10\lambda_0$. CPW = 20 for both of the two schemes.

FDTD (2, 4) scheme exhibits much better in tracing the curves of the benchmark date than the FDTD (2, 2) scheme. The performance of the FDTD (2, 2) scheme was poor involved in calculating RCS, especially for the backscattered RCS. And the hybrid FDTD (2, 4) scheme behaves much finer performance, it can been observed that the hybrid FDTD (2, 4) could improve the accuracy significantly maintaining the same CPW as the FDTD (2, 2) scheme. Figure 6 repeats the Figure 5 with the FDTD (2, 2) scheme run at CPW = 30 instead. However, the performance of the FDTD (2, 2) shown in Figure 6 is not much better than that shown in Figure 5. Furthermore, the computer resources that the two schemes cost have been compared. When CPW is 20, The memory cost of the two schemes are 16.7 GB. Although the memory cost of the FDTD (2, 2) scheme is the same as the hybrid FDTD (2, 4) scheme due to the same CPW, the accurate level is much worse than the hybrid FDTD (2, 4) scheme. More ever, if ones want to improve the accuracy of the FDTD (2, 2) scheme, the CPW must be large enough, which will lead to much more memory cost than the hybrid FDTD (2, 4) scheme. Such as when CPW is up to 30 for FDTD (2, 2) scheme, the memory cost is 48.4 GB, the performance of the scheme is still not as fine as that of hybrid FDTD (2, 4) scheme shown in Figure 6. The execution time of the two scheme are 14 hours and 33 minutes and 23 hours and 22 minutes when CPW is 20. Obviously, the hybrid

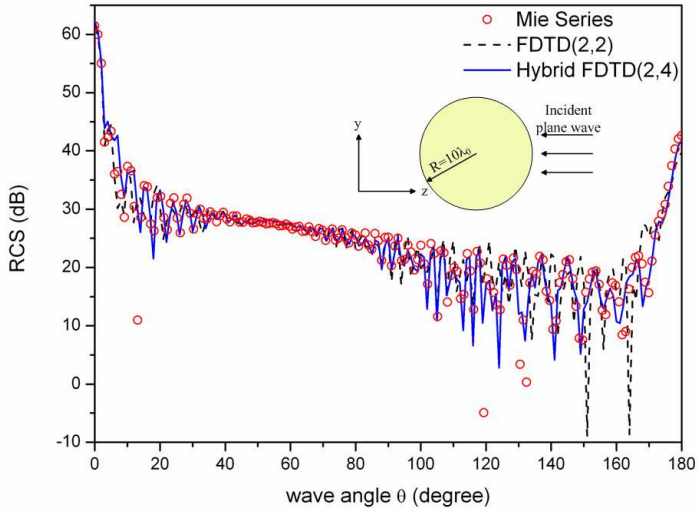

Figure 6. Copolarized RCS of dielectric sphere with radius $R = 10\lambda_0$. CPW = 20 for hybrid FDTD (2, 4) scheme, CPW = 30 for FDTD (2, 2) scheme.

FDTD (2, 4) have taken more execution times because of the more numbers of FLOPS than the FDTD (2, 2) scheme. Nevertheless, the execution time of the FDTD (2, 2) scheme would become longer as the increased CPW for better accurate level, which would result to more execution times. Such as when CPW equals to 30 shown in Figure 6, the execution time is nearly 58 hours. Unfortunately, the parallel computation technology has not been implemented in our work, if the technology would be applied in this work, the execution time would been reduced considerably, and the computational efficiency would become much higher.

5. CONCLUSION

In this paper, the hybrid FDTD (2, 4) scheme is proposed to analyzed the far field scattering problems. The scheme consists of both the classical FDTD (2, 2) scheme and the higher order FDTD (2, 4) scheme, and a few special FDTD (2, 2) scheme's cells in the scattered field region have been used as buffers to avoid that the larger FDTD (2, 4) stencils intrude inside the PML regions. Although there is phase-mismatching [25] at the interface between the FDTD (2, 2) and FDTD (2, 4) domain, the numerical results illustrate the proposed scheme

is more accuracy and more efficient referred to analyzing the RCS of electrically large targets compared to the classical FDTD (2, 2) scheme. It should been pointed that the proposed scheme is very easy to implement, usually, ones only need to add a few codes into the existing computer code for the classical Yee's scheme. In our future work, the parallel computation technology would been implement for the hybrid FDTD (2, 4) scheme to make the computational efficiency of the scheme much higher. However, the fit between the results obtained by the proposed method and Mie theory is not perfect, which is mainly due to the staircasing approximations of the surfaces of the dielectric cylinder and spheres. This problem will be deal with in the future work by implementing conformal technology into the proposed method in this paper.

REFERENCES

1. Ishimaru, A., Ed., *Wave Propagation and Scattering in Random Media*, 2nd edition, Academic, New York, 1978.
2. Yee, K. S., "Numerical solution of initial boundary value problems involving Maxwell' s equations in isotropic media," *IEEE Transactions on Antennas and Propagation*, Vol. 14, 302–307, 1966.
3. Taflove, A. and S. Hagness, *Computational Electromagnetics: The Finite-difference Time-domain Method*, 3nd Edition, Artech House, Boston, MA, 2005.
4. Taflove, A., K. R. Umashankar, and T. G. Jurgens, "Validation of FDTD modeling of the radar cross-section of three-dimensional structures spanning up to 9 wavelengths," *IEEE Transactions on Antennas and Propagation*, Vol. 33, 662–666, 1985.
5. Li, X., A. Taflove, and V. Backman, "Modified FDTD near-to-far-field transformation for improved backscattering calculation of strongly forward-scattering objects," *IEEE Antennas and Wireless Propagation Letters*, Vol. 4, 35–38, 2005.
6. Umashankar, K. R. and A. Taflove, "A novel method to analyze electromagnetic scattering of complex objects," *IEEE Transactions on Electromagnetic Compatibility*, Vol. 24, 397–405, 1982.
7. Shlager, K. L. and J. B. Schneider, "Comparison of the dispersion properties of several low-dispersion finite-difference time-domain algorithms," *IEEE Transactions on Antennas and Propagation*, Vol. 51, 642–653, 2003.
8. Nehrbass, J. W., J. O. Jevtc, and R. Lee, "Reducing the phase

error for finite-difference methods without increasing the order," *IEEE Transactions on Antennas and Propagation*, Vol. 46, 1194–1201, 1998.

9. Cole, J. B., "High-accuracy realization of the Yee algorithm using non-standard finite differences," *IEEE Transactions on Microwave Theory and Techniques*, Vol. 45, 991–996, 1997.
10. Kim, W.-T., I.-S. Koh, and J.-G. Yook, "3D isotropic dispersion (ID)-FDTD algorithm: Update equation and characteristics analysis," *IEEE Transactions on Antennas and Propagation*, Vol. 58, 1251–1259, 2010.
11. Lan, K., Y. Liu, and W. Lin, "Higher order (2, 4) scheme for reducing dispersion in FDTD algorithm," *IEEE Transactions on Electromagnetic Compatibility*, Vol. 41, 160–165, 1999.
12. Georgakopoulos, S. V., C. R. Birtcher, C. A. Balanis, and R. A. Renaut, "Higher-order finite-difference schemes for electromagnetic radiation, scattering, and penetration. Part 1: Theory," *IEEE Antennas and Propagation Magazine*, Vol. 44, 134–142, 2002.
13. Georgakopoulos, S. V., C. R. Birtcher, and C. A. Balanis, "Higher-order finite-difference schemes for electromagnetic radiation, scattering, and penetration, Part 2: Applications," *IEEE Antennas and Propagation Magazine*, Vol. 44, 92–101, 2002.
14. Abd El-Raouf, H. E., E. A. El-Diwani, A. E.-H. Ammar, and F. El-Hefnawi, "A low-dispersion 3-D second-order in time fourth-order in space FDTD scheme (M3d24)," *IEEE Transactions on Antennas and Propagation*, Vol. 52, 1638–1646, 2004.
15. Zygiridis, T. T. and T. D. Tsiboukis, "Low-dispersion algorithms based on the higher order (2, 4) FDTD method," *IEEE Transactions on Microwave Theory and Techniques*, Vol. 52, 1321–1327, 2004.
16. Zygiridis, T. T. and T. D. Tsiboukis, "A dispersion-reduction scheme for the higher order (2, 4) FDTD method," *IEEE Transactions on Magnetics*, Vol. 40, 1464–1467, 2004.
17. Hadi, M. F. and S. F. Mahmoud, "A high-order compact-FDTD algorithm for electrically large waveguide analysis," *IEEE Transactions on Antennas and Propagation*, Vol. 56, 2589–2598, 2008.
18. Georgakopoulos, S. V. and R. A. Renaut, "A hybrid forth-order FDTD utilizing a second-order FDTD subgrid," *IEEE Microwave and Wireless Components Letters*, Vol. 11, 462–464, 2001.
19. Fang, J., "Time domain finite difference computation for

Maxwell's equations," Ph.D. Dissertation, University of California, Berkeley, CA, USA, 1989.

20. Hadi, M. F., "A finite volumes-based 3-D low dispersion FDTD algorithm," *IEEE Transactions on Antennas and Propagation*, Vol. 55, 2287–2293, 2007.
21. Berenger, J. P., "A perfectly matched layer for the absorption of electromagnetic waves," *Journal of Computional Physics*, Vol. 114, 185–200, 1994.
22. Zygiridis, T. T. and T. D. Tsiboukis, "Development of higher order FDTD schemes with controllable dispersion error," *IEEE Transactions on Antennas and Propagation*, Vol. 53, 2952–2960, 2005.
23. Hadi, M. F. and M. Piket-May, "Modified FDTD (2, 4) scheme for modeling electrically large structures with high-phase accuracy," *IEEE Transactions on Antennas and Propagation*, Vol. 45, 254–264, 1997.
24. Ogurtsov, S. and S. V. Georgakopoulos, "FDTD schemes with minimal numerical dispersion," *IEEE Transactions on Advanced Packaging*, Vol. 32, 199–204, 2009.
25. Hadi, M. F. and R. K. Dib, "Phase-matching the hybrid FV24/S22 FDTD algorithm," *Progress In Electromagnetics Research*, Vol. 72, 307–323, 2007.